Arabian Journal of Chemistry (2022) **15**, 104372

King Saud University

**Arabian Journal of Chemistry**

www.ksu.edu.sa
www.sciencedirect.com

ORIGINAL ARTICLE

# Facile synthesis and characterization of β-cobalt hydroxide/hydrohausmannite/ramsdellitee/spertiniite and tenorite/cobalt manganese oxide/manganese oxide as novel nanocomposites for efficient photocatalytic degradation of methylene blue dye

**Ehab A. Abdelrahman [a,b,*], R.M. Hegazey [c], Sameh H. Ismail [d], Hesham H. El-Feky [b], Abdalla M. Khedr [e], M. Khairy [a,b], Alaa M. Ammar [f]**

[a] *Department of Chemistry, College of Science, Imam Mohammad Ibn Saud Islamic University (IMSIU), Riyadh 11623, Saudi Arabia*
[b] *Chemistry Department, Faculty of Science, Benha University, Benha 13518, Egypt*
[c] *Egyptian Petroleum Research Institute, Ahmed El Zumer Street, Nasr City, Hai Al-Zehour, Cairo 11727, Egypt*
[d] *Faculty of Nanotechnology for Postgraduate Studies, Cairo University, Sheikh Zayed Campus, 6th October City, Giza 12588, Egypt*
[e] *Chemistry Department, Faculty of Science, Tanta University, Tanta 31111, Egypt*
[f] *Chemistry Department, Faculty of Science, Suez Canal University, Ismailia 41522, Egypt*

Received 15 August 2022; accepted 15 October 2022
Available online 20 October 2022

**KEYWORDS**

New photocatalysts;
Methylene blue dye;
Precipitation;
Ignition

**Abstract** In this paper, our research team has synthesized new nanocomposites by simple precipitation/ignition method and using low-cost chemicals. Hence, β-cobalt hydroxide/hydrohausmannite/ramsdellitee/spertiniite and tenorite/cobalt manganese oxide/manganese oxide new nanocomposites were synthesized by precipitation of Mn(II)/Co(II)/Cu(II) solution using sodium hydroxide and ignition of precipitate at 700 °C for 3 hrs, respectively. The synthesized nanocomposites were characterized using different instruments such as energy dispersive X-ray spectroscopy (EDX), X-ray diffraction (XRD), field emission scanning electron microscope (FE-SEM), transmission elec-

* Corresponding author at: Department of Chemistry, College of Science, Imam Mohammad Ibn Saud Islamic University (IMSIU), Riyadh 11623, Saudi Arabia.
E-mail addresses: EAAAhmed@imamu.edu.sa, ehab.abdelrahman@fsc.bu.edu.eg (E.A. Abdelrahman).
Peer review under responsibility of King Saud University.

Production and hosting by Elsevier

https://doi.org/10.1016/j.arabjc.2022.104372

tron microscope (TEM), nitrogen gas sorption analyzer, and UV–vis spectrophotometer. Energy dispersive X-ray analysis revealed that the nanocomposite formed as a result of precipitation consists of copper, cobalt, manganese, and oxygen where the weight percentages are equal to 31.73, 27.01, 17.26, and 24 %, respectively. Also, the nanocomposite formed as a result of ignition consists of copper, cobalt, manganese, and oxygen where the weight percentages are equal to 31.26, 23.87, 14.56, and 30.31 %, respectively. Transmission electron microscope revealed that the nanocomposites formed as a result of precipitation and ignition consist of polyhedral and spherical shapes with an average diameter of 34.50 and 28.56 nm, respectively. The synthesized nanocomposites were used as new photocatalysts for the efficient degradation of methylene blue dye. 0.05 g of the synthesized nanocomposites degrade 100 % of 50 mL of 15 mg/L of methylene blue dye solution within 25 min in the presence of $H_2O_2$ under UV light.



## 1. Introduction

Energy and environmental pollution challenges are already becoming among the world's most difficult problems. Plastics, printing, textiles, and other industries use untreated synthetic organic dyes that are mixed with water sources. The environment and humans may be adversely affected by synthetic organic dyes (Tang et al., 2022; Xie et al., 2022). Methylene blue is among the industrial organic dyes. It is amongst the most often used dyes for wood, cotton, and silk. Excessive concentrations of methylene blue dye in the water supplies can cause a range of diseases, such as troubles with the respiratory and digestive tracts, as well as profuse sweating, vomiting, and nausea (Kenawy et al., 2022). Various treatment procedures, such as biological processes, chemical oxidation, membrane filtration, coagulation, and advanced oxidation processes, are frequently employed to get rid of various organic dyes (Bustos-Terrones et al., 2021; Ihaddaden et al., 2022; Ismail and Sakai, 2022; Javanbakht and Mohammadian, 2021; Kim et al., 2004; Subrahmanya et al., 2022). Advanced oxidation processes, for instance, have an enormous ability to control many kinds of pollution and can decrease the generation of secondary contaminants since they produce carbon dioxide and water. In the presence of proper wavelengths of light, superoxide anion and hydroxyl radical production can attack organic molecules in wastewater during the photocatalytic process. These organic molecules can be decomposed into non-hazardous substances (Alharbi and Abdelrahman, 2020; Hegazey et al., 2020). Several composites were used as photocatalysts to degrade the methylene blue dye such as Bi/Carbon nanotubes/$\alpha$-$Fe_2O_3$ nanocomposite (Manda et al., 2022), $MgSO_4$/g-$C_3N_4$ composite (Zeng et al., 2022), $ZnWO_4/SnS_2$ nanocomposite (Kumar et al., 2022), $\alpha$-$Fe_2O_3$/ZnO nanocomposite (Harijan et al., 2022), multi-walled carbon nanotube/$WO_3$ nanocomposite (Stan et al., 2022), multi-walled carbon nanotube/$TiO_2$ nanocomposite (Jiang et al., 2011), multi-walled carbon nanotube/ZnO nanocomposite (Chaudhary et al., 2018), multi-walled carbon nanotube/$SnO_2/TiO_2$ nanocomposite (Réti et al., 2013), and $WO_3/Cu_2O$ nanocomposite (Li et al., 2022). These nanocomposites reduce electron/hole recombination and thus increase the efficiency of photocatalytic degradation of the methylene blue dye (Harijan et al., 2022). However, most of these nanocomposites require expensive chemicals to prepare. The precipitation and/or ignition method has proven its efficiency in preparing many nanomaterials such as ferrimagnetic nanoparticles (Kumar and Gangawane, 2022), $CeO_2$ nanoparticles (Shibeshi et al., 2022), copper ferrite nanoparticles (Subha et al., 2022), zinc oxide nanoparticles (Mahmood et al., 2022), bismuth oxychloride nanoparticles (Puttaraju et al., 2022), $Co_3O_4$ nanoparticles (Nassar et al., 2017), NiO nanoparticles (Nassar et al., 2017), and CuO nanoparticles (Aly et al., 2015). So, in this paper, our research team has synthesized new nanocomposites by simple precipitation/ignition method and using low-cost chemicals. In this concern, β-cobalt hydroxide/hydro hausmannite/ramsdellitee/spertiniite and tenorite/cobalt manganese oxide/manganese oxide new nanocomposites were synthesized by precipitation of Mn(II)/Co(II)/Cu(II) solution using sodium hydroxide and ignition of precipitate at 700 °C for 3 hrs, respectively. The synthesized nanocomposites were characterized using different instruments such as energy dispersive X-ray spectroscopy (EDX), X-ray diffraction (XRD), field emission scanning electron microscope (FE-SEM), transmission electron microscope (TEM), nitrogen gas sorption analyzer, and UV–vis spectrophotometer. The synthesized nanocomposites were used as new photocatalysts for the degradation of methylene blue dye. Moreover, analytical factors affecting the degradation efficiency of methylene blue dye have been studied, such as pH, time, concentration of dye, and amount of catalyst.

## 2. Experimental

### 2.1. Chemicals

Copper(II) acetate monohydrate ($Cu(CH_3COO)_2{\cdot}H_2O$), cobalt (II) acetate tetrahydrate ($Co(CH_3COO)_2{\cdot}4H_2O$), manganese (II) acetate tetrahydrate ($Mn(CH_3COO)_2{\cdot}4H_2O$), sodium hydroxide (NaOH), methylene blue dye ($C_{16}H_{18}ClN_3S$), hydrogen peroxide ($H_2O_2$), and hydrochloric acid (HCl) were purchased from Sigma Aldrich Company (Purity = 99.99 % ) and utilized as received without further purification.

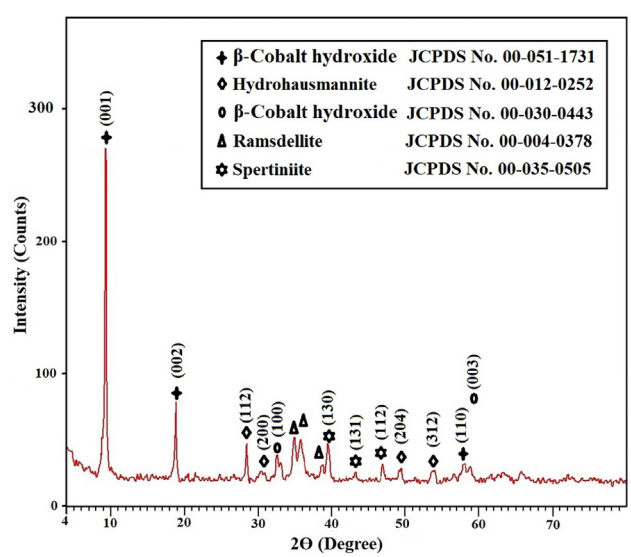


**Fig. 1** X-ray diffraction analysis of the nanocomposite formed as a result of precipitation using sodium hydroxide.

*2.2. Synthesis of nanocomposites*

10 g of copper(II) acetate monohydrate, 10 g of cobalt(II) acetate tetrahydrate, and 10 g of manganese(II) acetate tetrahydrate were dissolved in 300 mL of distilled water for obtaining the mixed metal solution. 11 g of sodium hydroxide was dissolved in 100 mL of distilled water. Then, the sodium hydroxide solution was added to the mixed metal solution drop by drop with constant stirring for 2 hrs. After that, the formed precipitate was filtered, washed with hot distilled water, and dried at 70 °C for 12 hrs. Furthermore, the dried precipitate was ignited at 700 °C for 3 hrs.

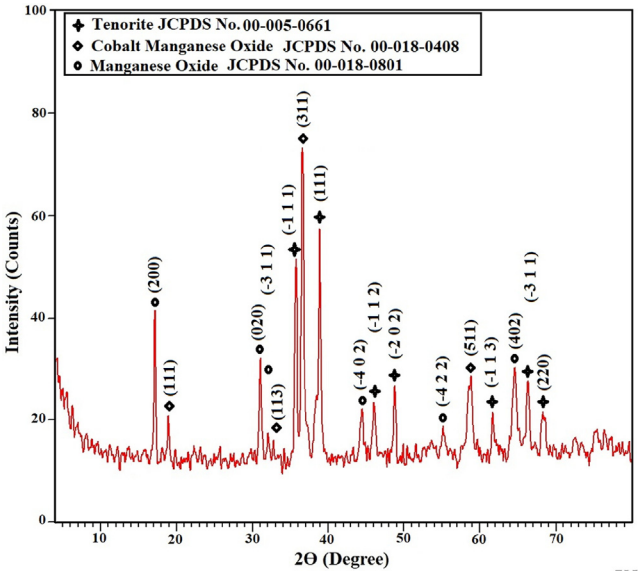


**Fig. 2** X-ray diffraction analysis of the nanocomposite formed as a result of ignition at 700 °C for 3 hrs.

*2.3. Characterization*

X-ray diffraction patterns of the synthesized nanocomposites were obtained utilizing a Bruker $D_8$ Advance X-ray diffractometer adopting copper target with $K_\alpha$ line have a wavelength equal to 0.15 nm. The surface morphology and EDX spectra of the synthesized nanocomposites were obtained utilizing a JSM-IT800 Schottky field emission scanning electron microscope (FE-SEM). The morphologies of the synthesized nanocomposites were obtained utilizing a Talos F200iS transmission electron microscope (TEM). The synthesized nanocomposites were degassed at 60 °C for 24 hrs then a nitrogen gas sorption analyzer (Quantachrome TouchWin, Austria, Graz) was utilized for the determination of the average pore radius, BET surface area, and total pore volume. The concentration of the methylene blue dye and energy gap of the synthesized nanocomposites were determined utilizing a Jasco V-670 UV–vis spectrophotometer. The maximum wavelength of methylene blue dye is 663 nm.

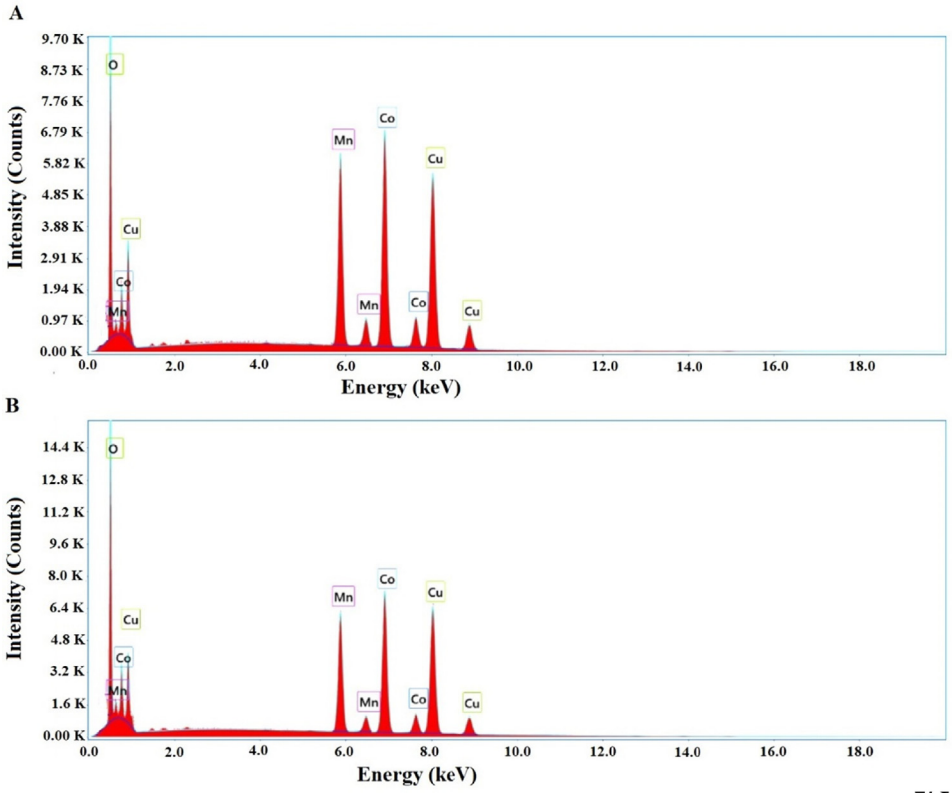


**Fig. 3** Energy dispersive X-ray analysis of the nanocomposites formed as a result of precipitation (A) and ignition (B).

*2.4. Photocatalytic degradation of methylene blue dye using the synthesized nanocomposites*

Photocatalytic degradation of methylene blue dye using the synthesized nanocomposites has been studied at different pH values (3–8) as follows: 0.05 g of the synthetic catalyst was added to 50 mL of a methylene blue dye solution with a concentration of 15 mg/L. Then, the catalyst/methylene blue dye mixture was stirred in a dark place for 2 hrs. After that, the catalyst/methylene blue dye mixture was exposed to ultraviolet rays, under stirring for 2 hrs, using a UV lamp (Wavelength = 254 nm, Power = 8 Watt, Length = 30 cm, Model G8W, Sylvania lighting, Japan) located 5 cm away from the beaker containing the catalyst/methylene blue dye mixture. The previous experimental steps were repeated but in the presence of 1 mL of 2 M of hydrogen peroxide solution.

Photocatalytic degradation of methylene blue dye using the synthesized nanocomposites has been studied at different UV irradiation time values (5–60 min) as follows: 0.05 g of the synthetic catalyst was added to 50 mL of a methylene blue dye solution with a concentration of 15 mg/L. It is worth noting that the pH of the methylene blue dye solution was adjusted to 8 before the addition of the catalyst. Then, the catalyst/methylene blue dye mixture was stirred in a dark place for 2 hrs. After that, the catalyst/methylene blue dye mixture was exposed to ultraviolet rays during stirring for different times. The previous experimental steps were repeated but in the presence of 1 mL of 2 M of hydrogen peroxide solution.

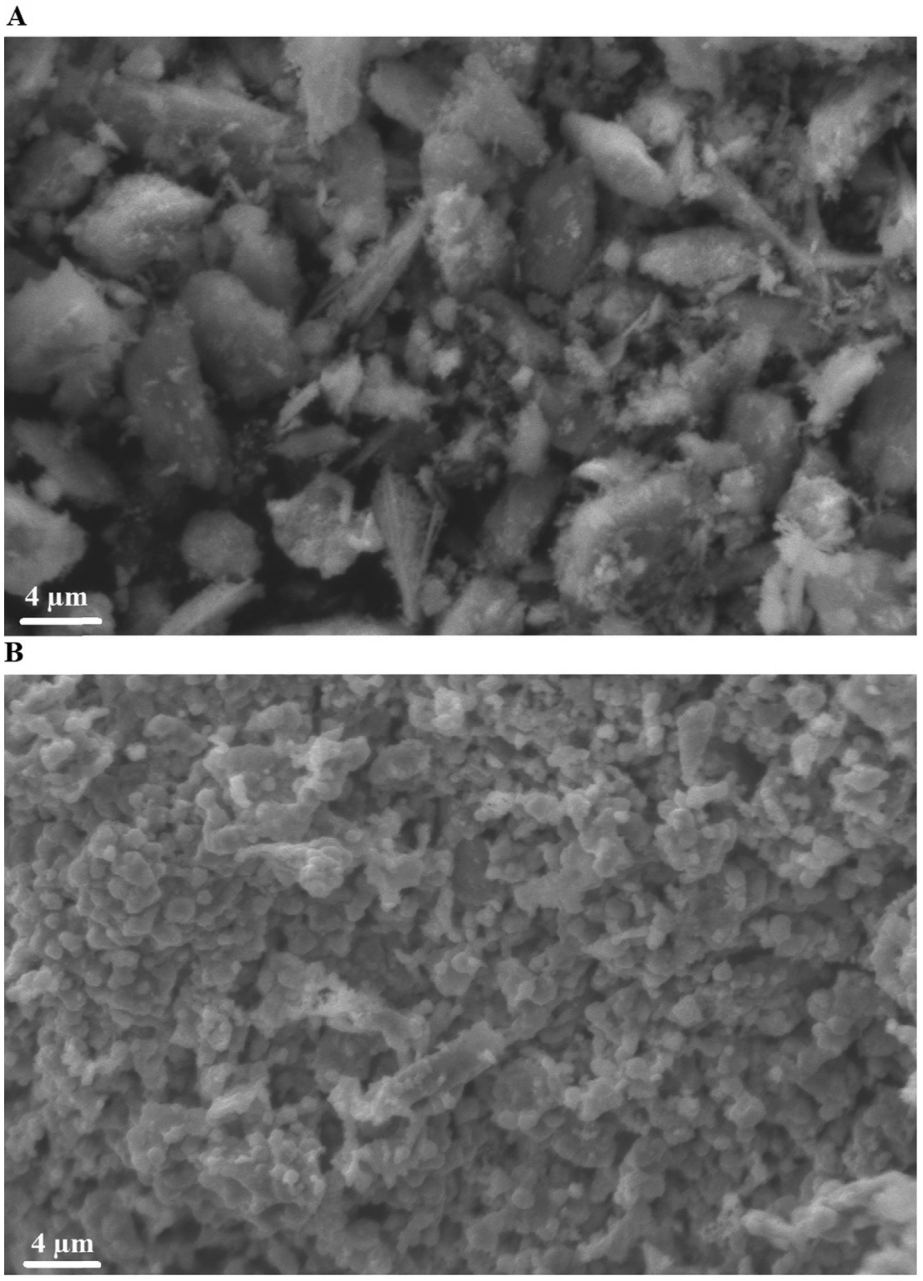


**Fig. 4** Scanning electron microscope analysis of the nanocomposites formed as a result of precipitation (A) and ignition (B).

Photocatalytic degradation of methylene blue dye using the synthesized nanocomposites has been studied using different amounts of catalysts (0.0125–0.2 g) as follows: A definite amount of the synthetic catalyst was added to 50 mL of a methylene blue dye solution with a concentration of 15 mg/L. It is worth noting that the pH of the methylene blue dye solution was adjusted to 8 before the addition of the catalyst. Then, the catalyst/methylene blue dye mixture was stirred in a dark place for 2 hrs. After that, the catalyst/methylene blue dye mixture was exposed to ultraviolet rays during stirring for 40 min and 25 min in the absence and presence of $H_2O_2$, respectively.

Photocatalytic degradation of different concentrations of methylene blue dye (5–30 mg/L) using the synthesized nanocomposites has been studied as follows: 0.05 g of the synthetic catalyst was added to 50 mL of a methylene blue dye solution. It is worth noting that the pH of the methylene blue dye solution was adjusted to 8 before the addition of the catalyst. Then, the catalyst/methylene blue dye mixture was stirred in a dark place for 2 hrs. After that, the catalyst/methylene blue dye mixture was exposed to ultraviolet rays during stirring for 40 min and 25 min in the absence and presence of $H_2O_2$, respectively.

The photodegradation efficiency (% P) of methylene blue dye was determined using Eq. (1).

$$\%P = \frac{A_0 - Ae}{A_o} \times 100 \quad (1)$$

$A_o$ (mg/L) is the concentration of the methylene blue dye after the end of its stirring period in a dark place. $A_e$ (mg/L) is the concentration of the methylene blue dye after the expiration of the period of stirring in the presence of ultraviolet rays. In order to study the effect of reusability, the photocatalysts are reformatted by washing them thoroughly with hot distilled water after each use. After that, photocatalysts were used 4 times to degrade the methylene blue dye in the same manner which previously mentioned.

## 3. Results and discussion

### 3.1. Characterization of the synthesized nanocomposites

X-ray diffraction analysis revealed that the nanocomposite formed as a result of precipitation using sodium hydroxide has an average crystallite size of 33.40 nm and consists of β-cobalt hydroxide (β-$Co(OH)_2$ as clarified from JCPDS No. 00-051-1731 and JCPDS No. 00-030-0443), hydrohausmannite

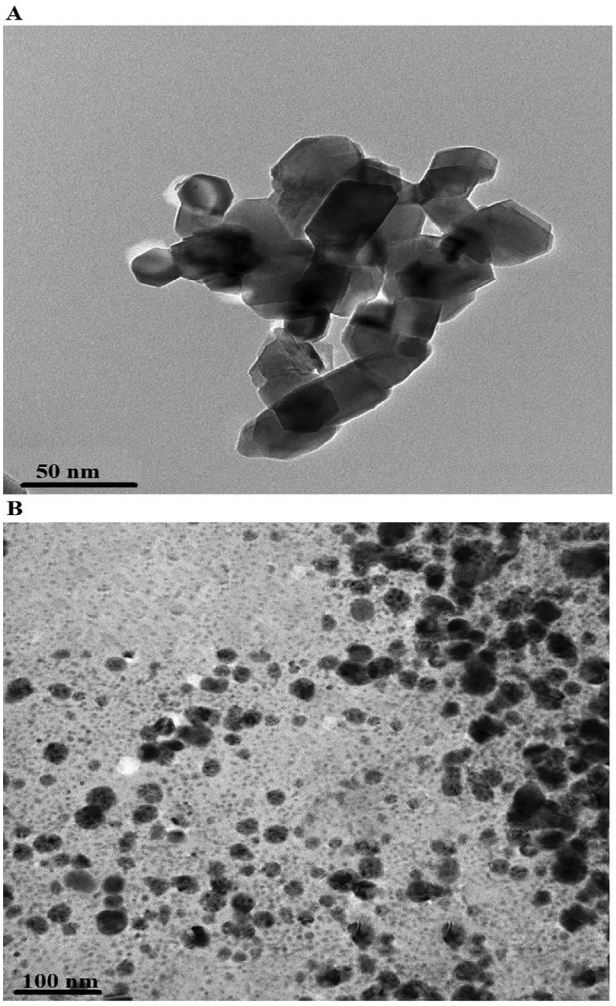


**Fig. 5** Transmission electron microscope analysis of the nanocomposites formed as a result of precipitation (A) and ignition (B).

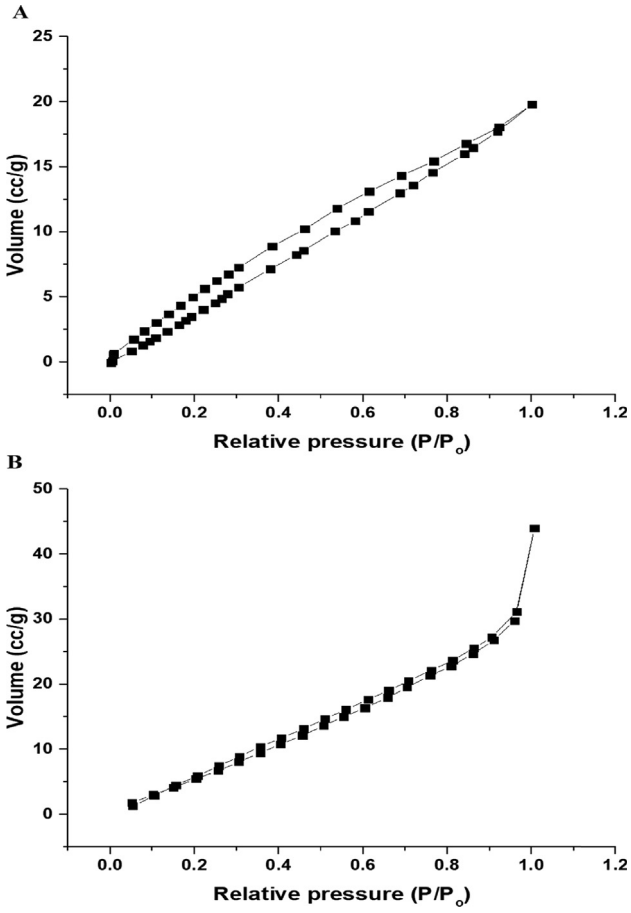


**Fig. 6** $N_2$ adsorption/desorption isotherms of the nanocomposites formed as a result of precipitation (A) and ignition (B).

(($Mn_{4-2x}Mn_x$) $Mn_8O_{16-x}(OH)_x$ as clarified from JCPDS No. 00–012-025), ramsdellitee ($MnO_2$ as clarified from JCPDS No. 00–004-0378), and spertiniite ($Cu(OH)_2$ as clarified from JCPDS No. 00–035-0505), as presented in Fig. 1. The miller indices of β-cobalt hydroxide at 2θ = 9.5°, 18.9°, and 58° are (001), (002), and (110), respectively. The miller indices of β-cobalt hydroxide at 2θ = 32.5° and 59° are (100) and (003), respectively. The miller indices of hydrohausmannite at 2θ = 28.7°, 30.9°, 49.2°, and 53.9° are (112), (200), (204), and (312), respectively. The miller indices of spertiniite at 2θ = 39.7°, 43.2°, and 47° are (130), (131), and (112), respectively.

X-ray diffraction analysis revealed that the nanocomposite formed as a result of ignition at 700 °C for 3 hrs has an average crystallite size of 24.28 nm and consists of tenorite (CuO as clarified from JCPDS No. 00-005-0661), cobalt manganese oxide ((Co,Mn) $(Co,Mn)_2O_4$ as clarified from JCPDS No. 00-018-0408), and manganese oxide ($Mn_5O_8$ as clarified from JCPDS No. 00-018-0801), as presented in Fig. 2. The miller indices of tenorite at 2θ = 35.5°, 38.7°, 46.3°, 48.8°, 61.5°, 66.2°, and 68.1° are (−111), (111), (−112), (−202), (−113), (−311), and (220), respectively. The miller indices of cobalt manganese oxide at 2θ = 18.5°, 32.9°, 36.4°, and 59° are (111), (113), (311), and (511), respectively. The miller indices of manganese oxide at 2θ = 18.1°, 31.2°, 31.9°, 44.3°, 55.1°, and 64.4° are (200), (020), (−311), (−402), (−422), and (402), respectively.

Energy dispersive X-ray analysis revealed that the nanocomposite formed as a result of precipitation using sodium hydroxide consists of copper, cobalt, manganese, and oxygen where the weight percentages are equal to 31.73, 27.01, 17.26, and 24 %, respectively, as shown in Fig. 3A. Also, energy dispersive X-ray analysis revealed that the nanocomposite formed as a result of ignition at 700 °C for 3 hrs consists of copper, cobalt, manganese, and oxygen where the weight percentages are equal to 31.26, 23.87, 14.56, and 30.31 %, respectively, as shown in Fig. 3B.

Scanning electron microscope analysis revealed that the nanocomposites formed as a result of precipitation using sodium hydroxide and ignition at 700 °C for 3 hrs consist of irregular and spherical shapes with an average diameter of 3.63 and 0.83 μm, as shown in Fig. 4A-B, respectively.

Transmission electron microscope analysis revealed that the nanocomposites formed as a result of precipitation using sodium hydroxide and ignition at 700 °C for 3 hrs consist of polyhedral and spherical shapes with an average diameter of 34.50 and 28.56 nm, as shown in Fig. 5A-B, respectively.

$N_2$ adsorption/desorption analyzer revealed that the isotherms of nanocomposites formed as a result of precipitation using sodium hydroxide and ignition at 700 °C for 3 hrs belong to type IV as shown in Fig. 6A-B, respectively (Abdelwahab et al., 2022; Khalifa et al., 2020). The BET surface area, total

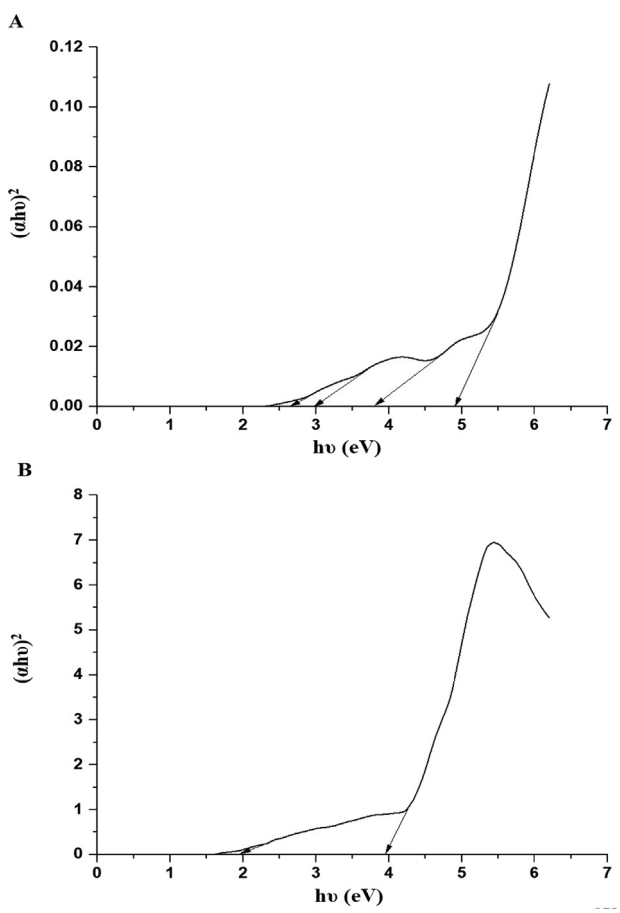


**Fig. 7** The plot of $(\alpha h\upsilon)^2$ versus hυ for the nanocomposites formed as a result of precipitation (A) and ignition (B).

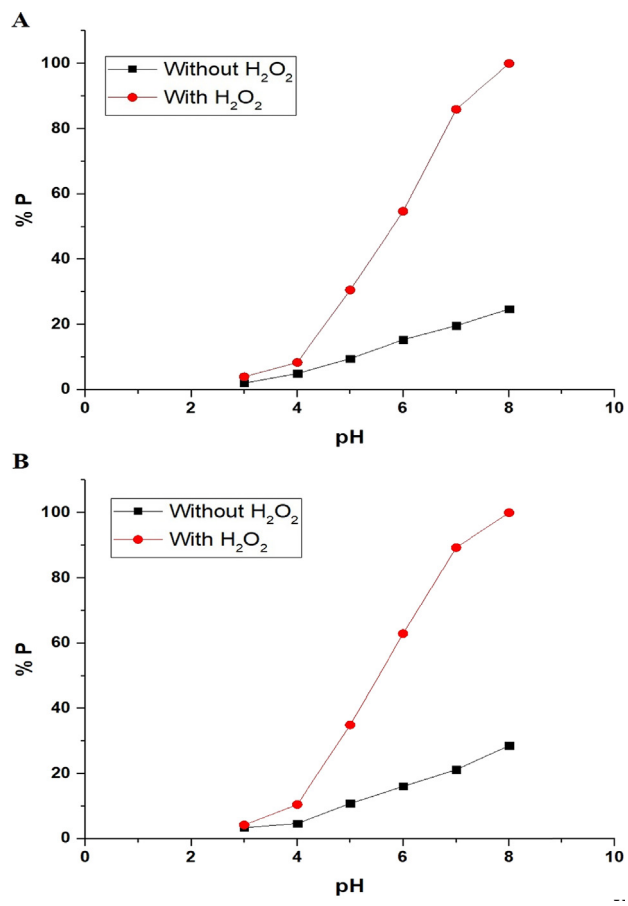


**Fig. 8** The effect of pH on the photodegradation efficiency (% P) of methylene blue dye using the nanocomposites formed as a result of precipitation (A) and ignition (B).

pore volume, and average pore size of the nanocomposite formed as a result of ignition at 700 °C for 3 hrs are 37.4716 $m^2/g$, 0.0415 cc/g, and 2.2148 nm, respectively. Also, the BET surface area, total pore volume, and average pore size of the nanocomposite formed as a result of precipitation using sodium hydroxide are 30.7931 $m^2/g$, 0.0307 cc/g, and 1.9938 nm, respectively.

By exploiting the spectrum of the synthesized nanocomposites in paraffin oil, the optical energy gap ($E_g$) of the synthesized nanocomposites was obtained using Eq. (2) (Alharbi and Abdelrahman, 2020).

$$(\alpha h\upsilon)^M = K_E(h\upsilon - E_g) \quad (2)$$

$K_E$, α, M are a constant, the absorption coefficient, and an integer based on the nature of the transition. M = 2 for direct allowed transitions, whereas M = 0.5 for indirect allowed transitions. Direct allowed transitions were dominant in the synthesized nanocomposites as displayed in Fig. 7A-B. The nanocomposite formed as a result of precipitation using sodium hydroxide has four values of energy gap, which are 2.62, 3.00, 3.85, and 4.95 eV. The nanocomposite formed as a result of ignition at 700 °C for 3 hrs has two values of energy gap, which are 1.97 and 3.94 eV.

### 3.2. Photocatalytic degradation of methylene blue dye

#### 3.2.1. Effect of pH

The effect of pH on the photodegradation efficiency (% P) of methylene blue dye, via the nanocomposites formed as a result of precipitation using sodium hydroxide and ignition at 700 °C for 3 hrs, can be seen in Fig. 8A-B, respectively. The figure indicates that pH = 8 helps to reach maximum degradation efficiency for methylene blue dye. The maximum photodegradation efficiency (% P) of methylene blue dye, using the nanocomposite formed as a result of precipitation using sodium hydroxide in the absence and presence of $H_2O_2$, is 24.70 and 100 %, respectively. Also, the maximum photodegradation efficiency (% P) of methylene blue dye, using the nanocomposite formed as a result of ignition at 700 °C for 3 hrs in the absence and presence of $H_2O_2$, is 28.57 and 100 %, respectively. It is noticeable that the photodegradation efficiency increases in the case of using hydrogen peroxide because it produces more hydroxyl free radicals when exposed to ultraviolet rays. The point of zero charge of the nanocomposites formed as a result of precipitation using sodium hydroxide and ignition at 700 °C for 3 hrs was determined as reported by Khalifa et al (Khalifa et al., 2020) and found

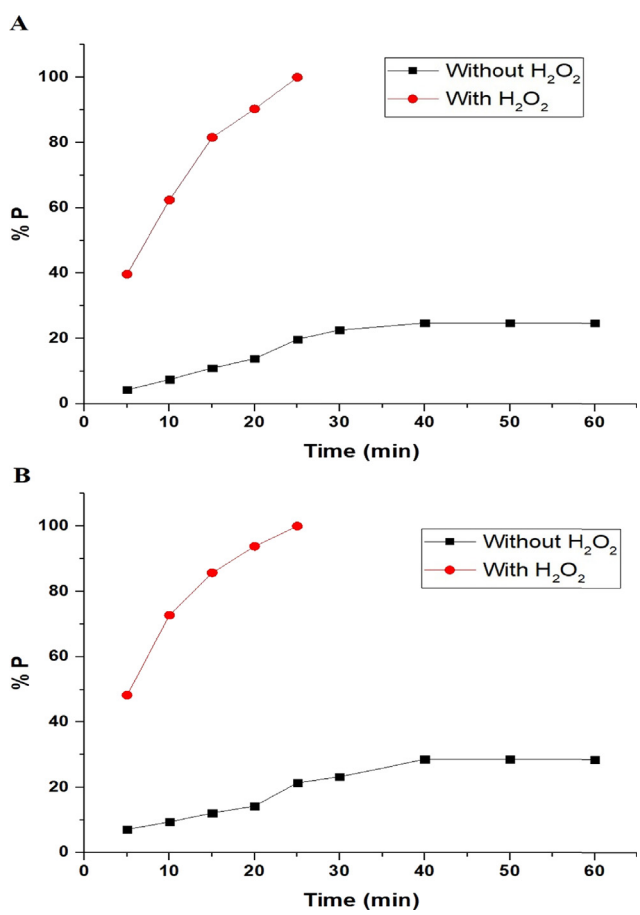


**Fig. 9** The effect of time on the photodegradation efficiency (% P) of methylene blue dye using the nanocomposites formed as a result of precipitation (A) and ignition (B).

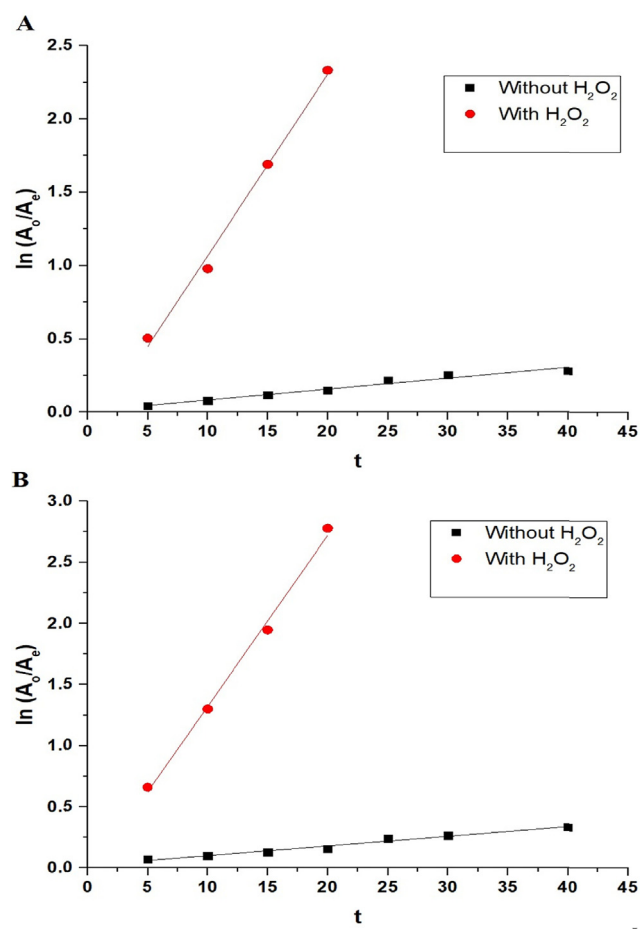


**Fig. 10** The plots of ln ($A_o/A_e$) versus irradiation time using the nanocomposites formed as a result of precipitation (A) and ignition (B).

to be 4.20 and 4.43, respectively. The electrostatic interactions between the negative catalyst surface and the cationic methylene blue dye at pH > $pH_{PZC}$ lead to an increase in the photodegradation efficiency of methylene blue dye. The electrostatic repulsions between the positive catalyst surface and the cationic methylene blue dye at pH < $pH_{PZC}$ lead to a decrease in the photodegradation efficiency of methylene blue dye (Abdelwahab et al., 2022).

### 3.2.2. Effect of time

The effect of UV irradiation time on the photodegradation efficiency (% P) of methylene blue dye, via the nanocomposites formed as a result of precipitation using sodium hydroxide and ignition at 700 °C for 3 hrs, can be seen in Fig. 9A-B, respectively. The figure indicates that time = 40 min and 25 min helps to reach maximum degradation efficiency for methylene blue dye using the synthesized nanocomposites in the absence and presence of $H_2O_2$, respectively. It is noticeable that the photodegradation efficiency, using the synthesized nanocomposites in the absence of hydrogen peroxide, did not change when increasing the time from 40 min to 60 min due to the saturation of active sites (Abdelwahab et al., 2022). Utilizing Eq. (3), the photocatalytic degradation process of methylene blue dye, via the nanocomposites formed as a result of precipitation by sodium hydroxide and ignition at 700 °C for 3 hrs, was found to follow the first-order kinetic model as seen in Fig. 10-A-B, respectively (Alharbi and Abdelrahman, 2020).

$$\ln(A_o/A_e) = K_F t \quad (3)$$

where, $K_F$ (1/min) is the constant of the first-order kinetic model, whereas t (min) is the UV irradiation time. The correlation coefficients ($R^2$) and $K_F$ values are listed in Table 1.

**Table 1** The constants of the first-order reaction of the degradation of methylene blue dye using the synthesized nanocomposites.

| Catalyst produced due to | $K_F$ (1/min) | | $R^2$ | |
|---|---|---|---|---|
| | Without $H_2O_2$ | With $H_2O_2$ | Without $H_2O_2$ | With $H_2O_2$ |
| Precipitation | 0.0075 | 0.1238 | 0.9553 | 0.9908 |
| Ignition | 0.0079 | 0.1401 | 0.9688 | 0.9934 |

### 3.2.3. Effect of amount of catalyst

The effect of the amount of photocatalyst on the photodegradation efficiency (% P) of methylene blue dye, via the nanocomposites formed as a result of precipitation using sodium hydroxide and ignition at 700 °C for 3 hrs, can be seen

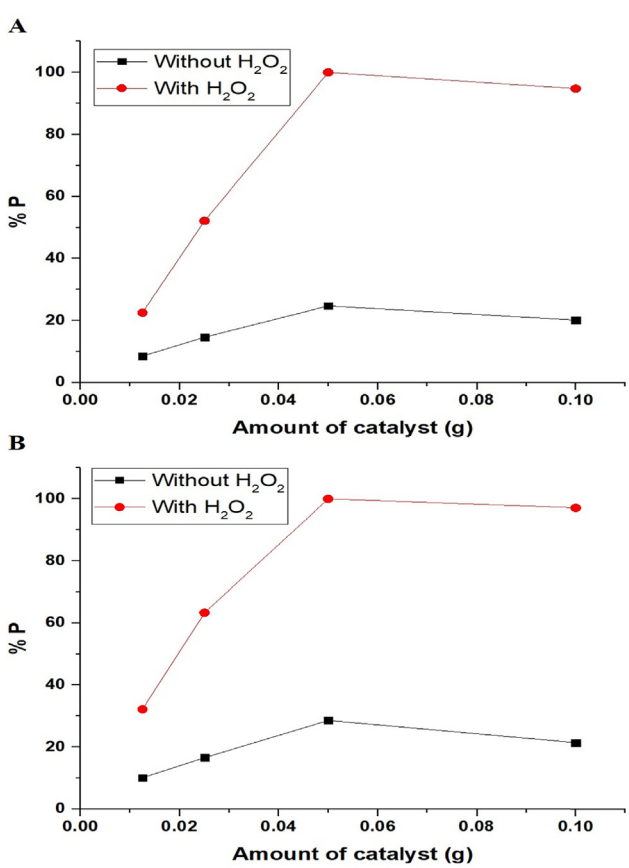


**Fig. 11** The effect of the amount of photocatalyst on the photodegradation efficiency (% P) of methylene blue dye using the nanocomposites formed as a result of precipitation (A) and ignition (B).

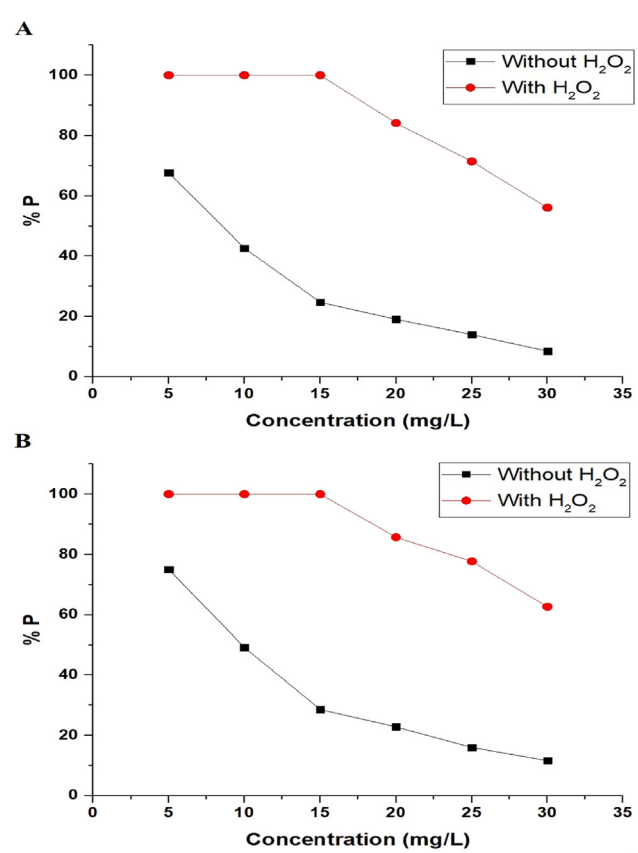


**Fig. 12** The effect of the initial concentration of methylene blue dye on the photodegradation efficiency (% P) using the nanocomposites formed as a result of precipitation (A) and ignition (B).

in Fig. 11A-B, respectively. The figure indicates that the amount of photocatalyst = 0.05 g helps to reach maximum degradation efficiency for methylene blue dye using the synthesized nanocomposites. This is a result of the rise in the number of photocatalyst particles, which boosts photon absorption. It is noticeable that the photodegradation efficiency decreases when increasing the amount of photocatalyst from 0.05 g to 0.10 g as a result of the scattering of incident UV light via the excess photocatalyst particles and the aggregation of the photocatalyst (Abdelwahab et al., 2022).

### 3.2.4. Effect of initial concentration of methylene blue dye

The effect of the initial concentration of methylene blue dye on the photodegradation efficiency (% P), via the nanocomposites formed as a result of precipitation using sodium hydroxide and ignition at 700 °C for 3 hrs, can be seen in Fig. 12A-B, respectively. It is noticeable that the photodegradation efficiency decreases when increasing the initial concentration of methylene blue dye as a result of the reduced path length of the UV photons arriving at the methylene blue dye solution, which decreases the photon absorption by the photocatalyst and consequently decreases the photocatalytic degradation (Abdelwahab et al., 2022).

### 3.2.5. Mechanism of photocatalytic degradation of methylene blue dye

Under the effect of UV irradiation, the photogenerated electrons stimulate to conduction band from the valence band, resulting in the creation of an electron/hole pair on the surface of the photocatalyst. The hydroxyl free radicals can be produced with the help of the holes, which react with the surface-bound water, whereas electrons of the conduction band can react with oxygen to form the superoxide radical anion of oxygen. The superoxide radical anion of oxygen can react with water to form hydroxyl free radicals. Under the effect of hydroxyl free radicals, the methylene blue dye can be decomposed into volatile gases such as $CO_2$ and $H_2O$ as clarified in Fig. 13 (Abdelwahab et al., 2022; Alharbi and Abdelrahman, 2020).

### 3.2.6. Effect of regeneration and reusability

The effect of the regeneration and reusability on the photodegradation efficiency (% P) of methylene blue dye, via the nanocomposites formed as a result of precipitation using sodium hydroxide and ignition at 700 °C for 3 hrs, can be seen in Fig. 14A-B, respectively. It is noticeable that the photodegradation efficiency is weakly affected when increasing

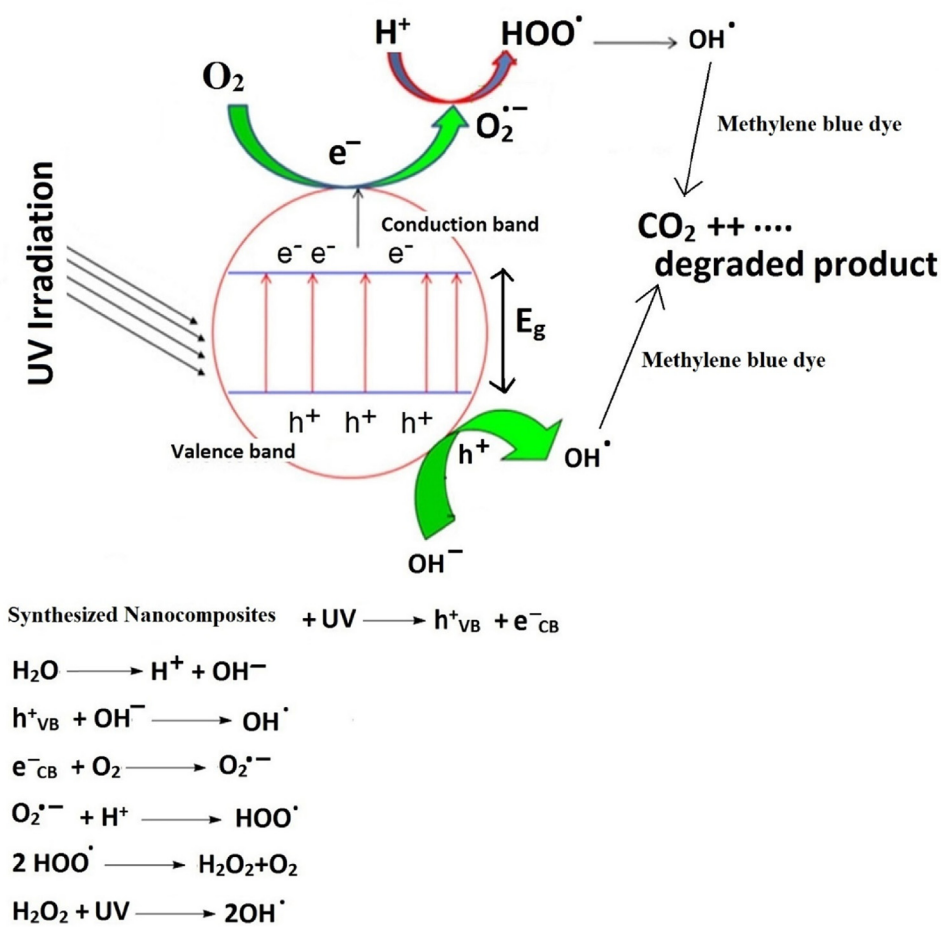


**Fig. 13** Proposed mechanism for the degradation of methylene blue dye using the synthesized nanocomposites.

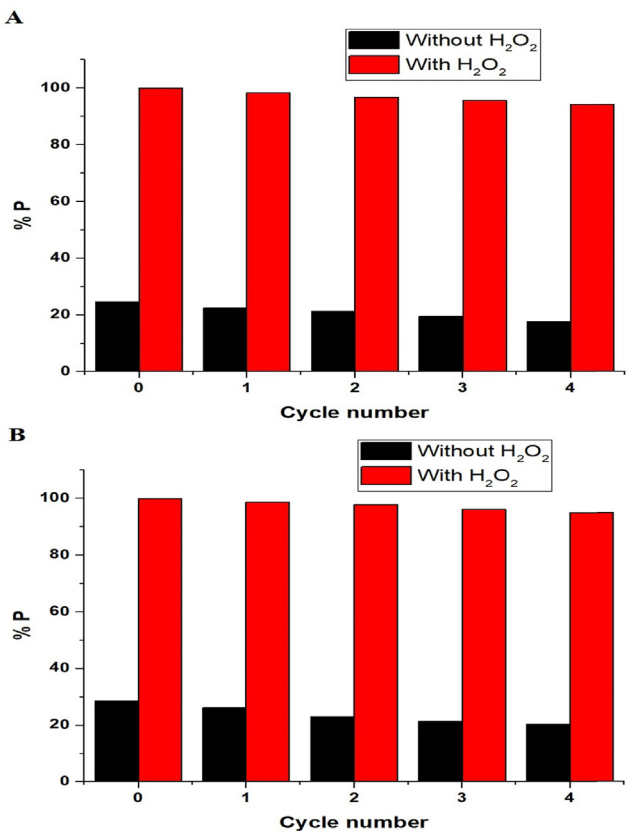


**Fig. 14** The effect of the regeneration and reusability on the photodegradation efficiency (% P) of methylene blue dye using the nanocomposites formed as a result of precipitation (A) and ignition (B).

the cycle number (Abdelwahab et al., 2022). Thus, the synthesized photocatalysts can be used many times without losing their efficiency.

### *3.2.7. Comparison of photocatalytic degradation of methylene blue dye using the synthesized nanocomposites with other photocatalysts in the literature*

As clearly seen in Table 2, the photocatalytic efficiency of methylene blue dye using the synthesized nanocomposites has been compared with that of other photocatalysts reported in the literature such as Bi/Carbon nanotubes/α-$Fe_2O_3$ nanocomposite (Manda et al., 2022), $MgSO_4$/g-$C_3N_4$ composite (Zeng et al., 2022), $ZnWO_4$/$SnS_2$ nanocomposite (Kumar et al., 2022), multi-walled carbon nanotube/$WO_3$ nanocomposite (Stan et al., 2022), and multi-walled carbon nanotube/$TiO_2$ nanocomposite (Jiang et al., 2011). The results demonstrated that the synthesized nanocomposites were superior to other photocatalysts in their capacity to rapidly degrade a significant volume and concentration of methylene blue dye.

## 4. Conclusions

Our research team has manufactured novel nanocomposites consist of copper, cobalt, manganese, and oxygen utilizing a simple precipitation/ignition technique and inexpensive ingredients. The synthesized nanocomposites were characterized using different instruments such as energy dispersive X-ray spectroscopy (EDX), X-ray diffraction (XRD), field emission scanning electron microscope (FE-SEM), transmission electron microscope (TEM), nitrogen gas sorption analyzer, and UV–vis spectrophotometer. 0.05 g of the produced nanocomposites degrade 100 % of 50 mL of 15 mg/L of methylene blue dye solution within 25 min in the presence of $H_2O_2$ under UV light.

## Declaration of Competing Interest

The authors declare that they have no known competing financial interests or personal relationships that could have appeared to influence the work reported in this paper.

## References

Abdelwahab, M.A., Rayes, S.M.E., Kamel, M.M., Ehab, A., 2022. Encapsulation of NiS and ZnS in analcime nanoparticles as novel nanocomposites for the effective photocatalytic degradation of orange G and methylene blue dyes Encapsulation of NiS and ZnS in analcime nanoparticles as novel nanocomposites for the effectiv. Int. J. Environ. Anal. Chem. 00, 1–18. https://doi.org/10.1080/03067319.2022.2100260.

Alharbi, A., Abdelrahman, E.A., 2020. Efficient photocatalytic degradation of malachite green dye using facilely synthesized hematite nanoparticles from Egyptian insecticide cans. Spectrochim. Acta - Part A Mol. Biomol. Spectrosc. 226,. https://doi.org/10.1016/j.saa.2019.117612 117612.

Aly, H.M., Moustafa, M.E., Nassar, M.Y., Abdelrahman, E.A., 2015. Synthesis and characterization of novel Cu (II) complexes with 3-substituted-4-amino-5-mercapto-1,2,4-triazole Schiff bases: A new route to CuO nanoparticles. J. Mol. Struct. 1086, 223–231. https://doi.org/10.1016/j.molstruc.2015.01.017.

Bustos-Terrones, Y.A., Hermosillo-Nevárez, J.J., Ramírez-Pereda, B., Vaca, M., Rangel-Peraza, J.G., Bustos-Terrones, V., Rojas-Valencia, M.N., 2021. Removal of BB9 textile dye by biological, physical,

**Table 2** Comparison between the photocatalytic efficiency of methylene blue dye using the synthesized nanocomposites and that of other photocatalysts in the literature.

| Catalyst | Amount of catalyst (g) | Concentration of dye (mg/L) | Volume of dye (mL) | % Degradation | Time (min) | Ref |
|---|---|---|---|---|---|---|
| Bi/Carbon nanotubes/α-$Fe_2O_3$ | 0.06 | 20 | 100 | 100 | 20 | (Manda et al., 2022) |
| $MgSO_4$/g-$C_3N_4$ | 0.03 | 20 | 50 | 98.45 | 90 | (Zeng et al., 2022) |
| $ZnWO_4$/$SnS_2$ | 0.03 | 20 | 50 | 99.60 | 75 | (Kumar et al., 2022) |
| Multi-walled carbon nanotube/$WO_3$ | 0.02 | 3.19 | 10 | 85.20 | 300 | (Stan et al., 2022) |
| Multi-walled carbon nanotube/$TiO_2$ | 0.1 | 30 | 100 | 92.5 | 60 | (Jiang et al., 2011) |
| Composite formed due to precipitation | 0.05 | 15 | 50 | 100 | 25 | This work |
| Composite formed due to ignition | 0.05 | 15 | 50 | 100 | 25 | This work |

chemical, and electrochemical treatments. J. Taiwan Inst. Chem. Eng. 121, 29–37. https://doi.org/10.1016/j.jtice.2021.03.041.

Chaudhary, D., Singh, S., Vankar, V.D., Khare, N., 2018. ZnO nanoparticles decorated multi-walled carbon nanotubes for enhanced photocatalytic and photoelectrochemical water splitting. J. Photochem. Photobiol. A Chem. 351, 154–161. https://doi.org/10.1016/j.jphotochem.2017.10.018.

Harijan, D.K.L., Gupta, S., Ben, S.K., Srivastava, A., Singh, J., Chandra, V., 2022. High photocatalytic efficiency of α-Fe2O3 -ZnO composite using solar energy for methylene blue degradation. Phys. B Condens. Matter 627,. https://doi.org/10.1016/j.physb.2021.413567 413567.

Hegazey, R.M., Abdelrahman, E.A., Kotp, Y.H., Hameed, A.M., Subaihi, A., 2020. Facile fabrication of hematite nanoparticles from Egyptian insecticide cans for efficient photocatalytic degradation of rhodamine B dye. J. Mater. Res. Technol. 9, 1652–1661. https://doi.org/10.1016/j.jmrt.2019.11.090.

Ihaddaden, S., Aberkane, D., Boukerroui, A., Robert, D., 2022. Removal of methylene blue (basic dye) by coagulation-flocculation with biomaterials (bentonite and Opuntia ficus indica). J. Water Process Eng. 49,. https://doi.org/10.1016/j.jwpe.2022.102952 102952.

Ismail, G.A., Sakai, H., 2022. Review on effect of different type of dyes on advanced oxidation processes (AOPs) for textile color removal. Chemosphere 291,. https://doi.org/10.1016/j.chemosphere.2021.132906 132906.

Javanbakht, V., Mohammadian, M., 2021. Photo-assisted advanced oxidation processes for efficient removal of anionic and cationic dyes using Bentonite/TiO2 nano-photocatalyst immobilized with silver nanoparticles. J. Mol. Struct. 1239,. https://doi.org/10.1016/j.molstruc.2021.130496 130496.

Jiang, G., Zheng, X., Wang, Y., Li, T., Sun, X., 2011. Photodegradation of methylene blue by multi-walled carbon nanotubes/TiO2 composites. Powder Technol. 207, 465–469. https://doi.org/10.1016/j.powtec.2010.11.029.

Kenawy, E.R., Tenhu, H., Khattab, S.A., Eldeeb, A.A., Azaam, M. M., 2022. Highly efficient adsorbent material for removal of methylene blue dye based on functionalized polyacrylonitrile. Eur. Polym. J. 169,. https://doi.org/10.1016/j.eurpolymj.2022.111138 111138.

Khalifa, M.E., Abdelrahman, E.A., Hassanien, M.M., Ibrahim, W.A., 2020. Application of Mesoporous Silica Nanoparticles Modified with Dibenzoylmethane as a Novel Composite for Efficient Removal of Cd(II), Hg(II), and Cu(II) Ions from Aqueous Media. J. Inorg. Organomet. Polym. Mater. 30, 2182–2196. https://doi.org/10.1007/s10904-019-01384-w.

Kim, T.H., Park, C., Yang, J., Kim, S., 2004. Comparison of disperse and reactive dye removals by chemical coagulation and Fenton oxidation. J. Hazard. Mater. 112, 95–103. https://doi.org/10.1016/j.jhazmat.2004.04.008.

Kumar, A., Gangawane, K.M., 2022. Effect of precipitating agents on the magnetic and structural properties of the synthesized ferrimagnetic nanoparticles by co-precipitation method. Powder Technol. 401,. https://doi.org/10.1016/j.powtec.2022.117298 117298.

Kumar, G., Kumar, J., Bag, M., Kumar Dutta, R., 2022. Solar light induced photocatalytic process for reduction of hexavalent chromium and degradation of tetracycline and methylene blue by heterostructures made of SnS2 nanoplates surface modified by ZnWO4 nanorods. Sep. Purif. Technol. 292,. https://doi.org/10.1016/j.seppur.2022.121040 121040.

Li, J., Guo, C., Li, L., Gu, Y., BoK-Hee, K., Huang, J., 2022. Construction of Z-scheme WO3-Cu2O nanorods array heterojunction for efficient photocatalytic degradation of methylene blue. Inorg. Chem. Commun. 138,. https://doi.org/10.1016/j.inoche.2022.109248 109248.

Mahmood, N.B., Saeed, F.R., Gbashi, K.R., Mahmood, U.S., 2022. Synthesis and characterization of zinc oxide nanoparticles via oxalate co-precipitation method. Mater. Lett. X 13,. https://doi.org/10.1016/j.mlblux.2022.100126 100126.

Manda, A.A., Elsayed, K.A., Ibrahim, U., Haladu, S.A., Alshammery, S., Altamimi, N.A., Al-otaibi, A.L., 2022. Enhanced photocatalytic degradation of methylene blue by nanocomposites prepared by laser ablation of Bi on CNT- α -$Fe_2O_3$ nanoparticles 155, 1–13. https://doi.org/10.1016/j.optlastec.2022.108430.

Nassar, M.Y., Aly, H.M., Abdelrahman, E.A., Moustafa, M.E., 2017. Synthesis, characterization, and biological activity of some novel Schiff bases and their Co(II) and Ni(II) complexes: A new route for Co3O4 and NiO nanoparticles for photocatalytic degradation of methylene blue dye. J. Mol. Struct. 1143, 462–471. https://doi.org/10.1016/j.molstruc.2017.04.118.

Puttaraju, T.D., Shashank, M., Raja Naika, H., Nagaraju, G., Manjunatha, M., 2022. Synthesis of bismuth oxychloride nanoparticles via co-precipitation method: Evaluation of photocatalytic activity. Mater. Today Proc. 62, 5533–5539. https://doi.org/10.1016/j.matpr.2022.04.333.

Réti, B., Péter, N., Dombi, A., Hernadi, K., 2013. Preparation of SnO2-TiO2/MWCNT nanocomposite photocatalysts with different synthesis parameters. Phys. Status Solidi Basic Res. 250, 2549–2553. https://doi.org/10.1002/pssb.201300076.

Shibeshi, P.T., Parajuli, D., Murali, N., 2022. Study of Fe-doped and glucose-capped CeO2 nanoparticles synthesized by co-precipitation method. Chem. Phys. 561,. https://doi.org/10.1016/j.chemphys.2022.111617 111617.

Stan, M., Toloman, D., Popa, A., Dan, M., Suciu, R.C., Macavei, S., Tripon, S.C., Chaiseeda, K., Pana, O., 2022. Facile synthesis of MWCNT-WO3 composites with enhanced photocatalytic degradation of methylene blue dye. Synth. Met. 288,. https://doi.org/10.1016/j.synthmet.2022.117117 117117.

Subha, A., Shalini, M.G., Sahu, B.N., Rout, S., Sahoo, S.C., 2022. Role of surface defects and anisotropy variation on magnetic properties of copper ferrite nanoparticles prepared by co-precipitation method. Mater. Chem. Phys. 286,. https://doi.org/10.1016/j.matchemphys.2022.126212 126212.

Subrahmanya, T.M., Widakdo, J., Mani, S., Austria, H.F.M., Hung, W.S., H K, M., Nagar, J.K., Hu, C.C., Lai, J.Y., 2022. An eco-friendly and reusable syringe filter membrane for the efficient removal of dyes from water via low pressure filtration assisted self-assembling of graphene oxide and SBA-15/PDA. J. Clean. Prod. 349, 131425. https://doi.org/10.1016/j.jclepro.2022.131425.

Tang, X., Tang, R., Xiong, S., Zheng, J., Li, L., Zhou, Z., Gong, D., Deng, Y., Su, L., Liao, C., 2022. Application of natural minerals in photocatalytic degradation of organic pollutants: A review. Sci. Total Environ. 812,. https://doi.org/10.1016/j.scitotenv.2021.152434 152434.

Xie, K., Fang, J., Li, L., Deng, J., Chen, F., 2022. Progress of graphite carbon nitride with different dimensions in the photocatalytic degradation of dyes: A review. J. Alloys Compd. 901. https://doi.org/10.1016/j.jallcom.2021.163589.

Zeng, G., Duan, M., He, J., Ge, F., Wang, W., 2022. Sulfate doped graphitic carbon nitride with enhanced photocatalytic activity towards degradation of methylene blue. Mater. Lett. 309,. https://doi.org/10.1016/j.matlet.2021.131310 131310.